

The Universe is at Most 88% Neutral at $z = 10.6$

SEAN BRUTON ¹, YU-HENG LIN ^{1,2}, CLAUDIA SCARLATA ^{1,2} AND MATTHEW J. HAYES ³

¹*Minnesota Institute for Astrophysics, University of Minnesota,
116 Church St SE, Minneapolis, MN 55455, USA*

²*School of Physics and Astronomy, University of Minnesota,
116 Church St SE, Minneapolis, Minnesota 55455, USA*

³*Stockholm University, Department of Astronomy and Oskar Klein Centre for Cosmoparticle Physics, AlbaNova University Centre,
SE-10691, Stockholm, Sweden*

(Received March 8, 2023; Revised May 5, 2023; Accepted May 15, 2023)

Submitted to ApJL

ABSTRACT

Recent observations of GN-z11 with JWST have revealed a Ly α emission line with an equivalent width of $18 \pm 2 \text{ \AA}$. At $z = 10.6$, this galaxy is expected to lie in the heart of reionization. We use a series of inhomogeneous reionization simulations to derive the distribution of the Ly α EW after traveling through the neutral intergalactic medium with varying average neutral gas fraction, x_{HI} . We use these distributions to place an upper limit of $x_{\text{HI}} < 0.88$ at $z = 10.6$ at 95% confidence level. We compare our upper limit to different reionization history models, which include the recently identified enhancement at the bright end of the luminosity function at $z > 8$. We find that models in which faint galaxies have higher escape fraction compared to bright galaxies are favored by the new data.

Keywords: reionization, galaxies: high-redshift

1. INTRODUCTION

In less than a year, *JWST* has revolutionized our knowledge of the very-high-redshift universe, spectroscopically confirming and photometrically identifying galaxy candidates as early as only a few hundred million years after the Big Bang (Schaerer et al. 2022; Brinchmann 2022; Finkelstein et al. 2022; Curtis-Lake et al. 2023; Cameron et al. 2023; Tang et al. 2023). Recently, Bunker et al. (2023) presented the spectroscopic confirmation of the Lyman-break galaxy candidate GN-z11. Using multiple rest-frame optical and UV emission lines, the redshift of GN-z11 was measured to be $z = 10.603 \pm 0.0013$, currently the highest known from emission lines for a likely star-forming galaxy (see discussion in Bunker et al. (2023)).

At redshift well above 10, GN-z11 is expected to be embedded in a largely neutral universe, as inferred from

a number of available data at $z \lesssim 8$ (e.g., Fan et al. 2006; McGreer et al. 2011, 2015; Ono et al. 2012; Schroeder et al. 2013; Choudhury et al. 2015; Greig et al. 2016; Mason et al. 2018a, 2019; Greig et al. 2019; Hoag et al. 2019; Jung et al. 2020). Inferring from lower-redshift observational studies suggests that the universe volume weighted neutral fraction (x_{HI}) is well above 90% at $z \gtrsim 10$, although no observational constraints currently exist at such early epochs. The spectrum of GN-z11 offers the unique opportunity to understand the state of the diffuse hydrogen at $z > 10$. Indeed, the spectrum reveals the presence of a strong Ly α emission line, with a rest-frame equivalent width (EW) of $18 \pm 2 \text{ \AA}$, and a velocity shift of the Ly α with respect to systemic velocity of $\Delta v_{\text{Ly}\alpha} \approx 550 \text{ km s}^{-1}$. This implies that GN-z11 resides in an ionized bubble, perhaps not surprising given that it is one of the brightest galaxies known at $z > 10$.

Ly α emission has been used extensively to place constraints on reionization. Ly α is a resonant transition in neutral hydrogen and is expected to completely disappear from the spectra of high-redshift galaxies when these are embedded in a fully neutral intergalactic

medium (IGM; [Dijkstra 2014, 2017](#)). The evolution of the absolute number density of Ly α emitters has been used to constrain the timeline of reionization (e.g., [Rhoads & Malhotra 2001; Malhotra & Rhoads 2004, 2006; Hu et al. 2019; Wold et al. 2021; Morales et al. 2021; Ning et al. 2022](#)). However, because Ly α is the byproduct of star-formation, its disappearance cannot be uniquely interpreted as signaling a completely neutral IGM. Studies of the reionization history of the universe are now often based on relative properties, e.g., on the relative fraction of Ly α emitters among star-forming galaxies ([Stark et al. 2010; Pentericci et al. 2011; Jung et al. 2018](#)), on the Ly α equivalent width distribution ($EW_{Ly\alpha}$; [Mason et al. 2018b; Hoag et al. 2019; Whitler et al. 2020](#)), or on the clustering of Ly α emitters ([Ouchi et al. 2010; Sobacchi & Mesinger 2015; Ouchi et al. 2018; Yoshioka et al. 2022](#)). Additionally, the environment in which a galaxy resides has an impact on the visibility of Ly α . A galaxy located within a region of the universe previously ionized by either itself, or a previous generation of stars, i.e., residing in what are commonly referred to as “ionized bubbles,” would be more likely to show Ly α in emission because Ly α photons would have time to redshift out of resonance before encountering the neutral IGM. The probability of observing Ly α emission then depends on the size of the ionized bubbles and the Ly α velocity shifts with respect to the IGM.

In this paper, we use the observations of GN-z11 to constrain x_{HI} at $z = 10.6$. Specifically, we use a set of simulations to forward model the evolution of the Ly α EW distribution in the presence of an increasingly neutral IGM and use these distributions to construct the likelihood of observing a galaxy with the observed $EW_{Ly\alpha}$ and M_{UV} properties as GN-z11.

The structure of the paper is as follows. In [Section 2](#), we postprocess 21cmFast simulations to create a model of Lyman- α emitters (LAEs). We then present our inference model. In [Section 3](#), we explore the implication of our result for the reionization history and discuss how the result depends on the assumptions. Finally we conclude in [Section 4](#). We assume a Λ CDM cosmology with $H_0 = 67.66 \text{ km s}^{-1} \text{ Mpc}^{-1}$ ([Planck-Collaboration et al. 2020](#)).

2. MODELING

The end goal of our modeling is to make an inference on the global neutral fraction of the universe, x_{HI} , at $z = 10.6$, in light of the fact that we observe one LAE with $EW_{Ly\alpha} = 18 \pm 2 \text{ \AA}$. To estimate x_{HI} , we will use a hierarchical Bayesian approach, similar to the one used in [Bruton et al. \(2023\)](#) and [Mason et al. \(2018b\)](#). We will populate a series of large inhomogenous reionization

simulations with LAEs and calculate the distribution of the $EW_{Ly\alpha}$ after transmission through the IGM of different ionization fractions.

2.1. Populating a Reionization Simulation with LAEs

Our model is built on the backbone of 21cmFastv2 ([Mesinger & Furlanetto 2007; Mesinger et al. 2011, 2016](#)), a seminumerical code that combines excursion set formalism and perturbation theory to create simulations of the universe throughout reionization. We use nine simulations with a volume average neutral fraction varying between $x_{HI}=0.01$ to $x_{HI}=0.92$, each 4.1 Gpc^3 in volume. When modeling the evolution of x_{HI} , 21cmFast takes into account recombinations, photoheating star-formation suppression, supernova feedback, and radiation. For each dark matter halo of mass, M_h , 21cmFast computes the integrated Ly α optical depth as a function of the velocity offset from line center. The simulations naturally account for the evolving presence of ionized bubbles around galaxies of different masses and residing in different environments.

In what follows, we define the emergent Ly α ($Ly\alpha_{\text{emer}}$), as the Ly α line luminosity escaping from the interstellar and circumgalactic medium of a galaxy, while the Ly α observed after passing through the IGM is referred to as transmitted Ly α ($Ly\alpha_{\text{tran}}$). To assign an emergent Ly α to a dark matter halo, we follow [Bruton et al. \(2023\)](#). Briefly, after using the M_h - M_{UV} relation from [Mason et al. \(2015\)](#) to assign an M_{UV} magnitude to each halo, we use the $EW_{Ly\alpha}$ - M_{UV} probability distribution from [Mason et al. \(2018a\)](#), calibrated with [De Barros et al. \(2017\)](#) observations, to randomly draw the emergent $EW_{Ly\alpha}$ for each halo. This is discussed in more detail in the following paragraph. The emergent Ly α line profile shape is assumed to be a truncated Gaussian, with velocity offset and Full-Width-Half-Maximum (FWHM) dependent on Ly α luminosity. The velocity offset scales linearly with the log of the Ly α luminosity (see [Bruton et al. \(2023\)](#) for more details), and we set FWHM equal to velocity offset, which is consistent with the findings in [Verhamme et al. \(2018\)](#), wherein they fit the relation between observed low- and high- z LAEs’ velocity offsets and FWHMs. They find the empirical relation to be consistent with the one-to-one relation predicted from radiation transfer modeling. We also note that [Hayes & Scarlata \(2023\)](#) find, through a Bayesian hierarchical inference model, that GN-z11’s intrinsic red wing Ly α emission has a velocity offset of 400 km s^{-1} and a FWHM of 433 km s^{-1} , consistent with the one-to-one. Finally, we use the line profiles, together with the velocity dependent optical depths of

$\text{Ly}\alpha$, to calculate the $\text{Ly}\alpha$ transmission, $T = \frac{\text{Ly}\alpha_{\text{tran}}}{\text{Ly}\alpha_{\text{emer}}}$, and the transmitted $\text{EW}_{\text{Ly}\alpha}$ as $\text{EW}_{\text{Ly}\alpha}^{\text{tran}} = T \times \text{EW}_{\text{Ly}\alpha}^{\text{emer}}$.

Our analysis rests on the assumption that the distribution of emergent $\text{EW}_{\text{Ly}\alpha}$ at $M_{\text{UV}} = -21.5$ does not change with redshift. For a generic M_{UV} , this distribution takes the form, from Mason et al. (2018a),

$$p(\text{EW}_{\text{Ly}\alpha}^{\text{emer}} | M_{\text{UV}}) = \frac{A(M_{\text{UV}})}{W_c(M_{\text{UV}})} e^{-\frac{\text{EW}_{\text{Ly}\alpha}}{W_c(M_{\text{UV}})}} H(\text{EW}_{\text{Ly}\alpha}) + [1 - A(M_{\text{UV}})]\delta(\text{EW}_{\text{Ly}\alpha}) \quad (1)$$

where $H(\text{EW}_{\text{Ly}\alpha})$ is the Heaviside step function and $\delta(\text{EW}_{\text{Ly}\alpha})$ is the Dirac delta function. The parameter A accounts for the fraction of galaxies that do not emit $\text{Ly}\alpha$ and W_c determines the exponential decline of the probability distribution function toward larger $\text{EW}_{\text{Ly}\alpha}$. Both parameters are functions of M_{UV} ; the general behavior is that brighter galaxies are more likely to be nonemitters and have a stronger exponential cutoff so that UV bright galaxies are less likely to have large $\text{EW}_{\text{Ly}\alpha}$. In Figure 1 we show the MUSE Hubble Ultra Deep Field (HUDF) Survey measurements of the average emergent $\text{EW}_{\text{Ly}\alpha}$ at different redshifts as a function of M_{UV} (Hashimoto et al. 2017), $z \sim 6$ observations from De Barros et al. (2017), and the prediction of our model. We apply an observed flux lower limit $> 8 \times 10^{-19} \text{erg s}^{-1}$ for $\text{Ly}\alpha$ to match the selection limit in the MUSE survey (the flux limit in the De Barros et al. (2017) data is similar at $2.2 \times 10^{-18} \text{erg s}^{-1}$ across the entire wavelength range, deeper in wavelength ranges without skylines).

We limit to data to $z \lesssim 6$, to limit the impact of the transmission through the IGM and isolate the effects of the interstellar and circumgalactic medium. This permits a comparison between $\text{EW}_{\text{Ly}\alpha}$ distributions at different redshifts to see if emergent $\text{EW}_{\text{Ly}\alpha}$ is independent of redshift. The comparison in Figure 1 confirms that there is no evidence of evolution in the median emergent $\text{EW}_{\text{Ly}\alpha}$ from $z = 3.6$ to $z = 4.9$, and weak evidence of evolution from $z = 4.9$ to $z = 6.0$, a redshift range corresponding to 800 million years. We note that a partially neutral IGM at $z = 6$ would remove LAEs with weak $\text{EW}_{\text{Ly}\alpha}$ from the observations and thus bias the distribution to be higher, and that the universe may not be fully ionized by $z = 6$ (Qin et al. 2021).

Still, we test the impact of the intrinsic $\text{EW}_{\text{Ly}\alpha}$ distribution by adopting a different exponential cutoff strength, W_c , for our intrinsic $\text{EW}_{\text{Ly}\alpha}$ distribution and redo our inference. For $M_{\text{UV}} = -21.5$, $W_c = 19$, as fit from the De Barros et al. (2017) data. As a test, we weaken the exponential cutoff, setting $W_c = 43$, which, allowing galaxies to take on $\text{EW}_{\text{Ly}\alpha}$ values greater than

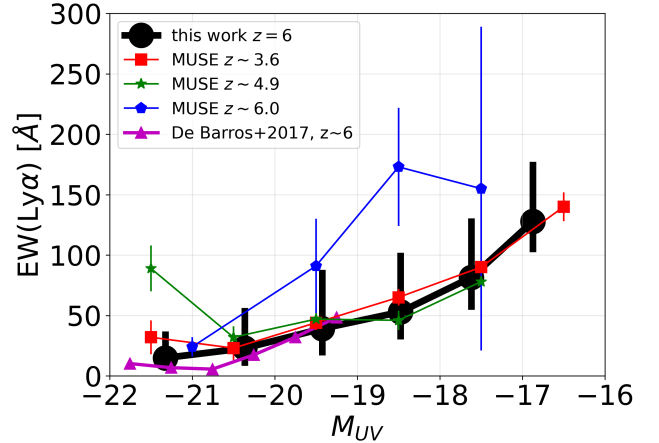


Figure 1. $\text{EW}(\text{Ly}\alpha)$ as a function of M_{UV} . The red squares, green stars, and blue pentagons are the measurements from the MUSE HUDF survey at redshift $z = 3.6$, 4.9, and 6.0, respectively. The magenta triangles are the median measurements from De Barros et al. (2017). The black circles are the results from our model, after matching the MUSE HUDF survey flux limit.

the GN-z11 value of 18\AA more easily, decreases the probability of having a galaxy with an $\text{EW}_{\text{Ly}\alpha}$ of 18\AA by $\approx 20\%$. When redoing the inference with this new distribution, we infer the same 95% upper limit on x_{HI} . This is an extremely different intrinsic $\text{EW}_{\text{Ly}\alpha}$ distribution, but the impact on the inferred value of x_{HI} is negligible. This shows that even if there is strong evolution in the intrinsic $\text{EW}_{\text{Ly}\alpha}$ distribution toward $z = 10.6$ allowing galaxies to have larger $\text{EW}_{\text{Ly}\alpha}$, its impact on our result will be small.

The $\text{Ly}\alpha$ transmission through an inhomogeneous IGM, particularly in the case of a highly neutral IGM, changes the $\text{EW}_{\text{Ly}\alpha}$ distribution, which is no longer well described by Equation 1. This is demonstrated in Figure 2, where we show $p(\text{EW}_{\text{Ly}\alpha}^{\text{tran}} | M_{\text{UV}} = -21.5, x_{\text{HI}})$ for two values of x_{HI} . For the highly neutral universe with $x_{\text{HI}} = 0.9$, the probability distribution function (PDF) of the transmitted $\text{EW}_{\text{Ly}\alpha}$ can no longer be modeled with the first term in Eq. 1. The observed excess of high-EW LAEs compared to the prediction from the ionized universe is a direct result of the inhomogeneity of the reionization process. Some galaxies reside in ionized bubbles, and their $\text{Ly}\alpha_{\text{emer}}$ is not very attenuated by the IGM. This results in a distribution of $\text{EW}_{\text{Ly}\alpha}$ that does not follow an exponential decline. This also highlights an important aspect of our simulations—the LAEs reside in a variety of local neutral fractions, which may differ from the global neutral fraction. However, when these LAEs are taken in conglomerate, the probability of having a given $\text{EW}_{\text{Ly}\alpha}$ is dependent on the global neutral fraction, not the local neutral fraction. Thus,

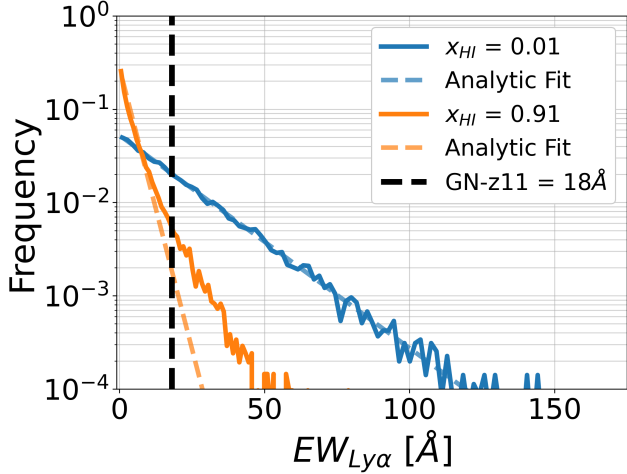


Figure 2. The probability of $EW(Ly\alpha)$ for varying values of x_{HI} , given that the galaxy has $Ly\alpha$ emission (i.e. excluding nonemitters). The solid lines are empirically taken from the simulation after IGM attenuation—the dashed lines are an attempt to fit the first term of Eq. 1 to the distribution. The fit fails when the universe is partially neutral because there is excess probability of having high $EW_{Ly\alpha}$ compared to an exponential cutoff.

the inference arising from this probability yields the global value, rather than a local value. Seeing as we have only one object to feed into our inference, we expect the posterior to be weakly constrained; more objects, probing more lines of sight, would be much more constraining.

2.2. Hierarchical Bayesian Inference of x_{HI}

Using Bayes' theorem, we write the x_{HI} posterior

$$p(x_{HI} | EW_{Ly\alpha}^{obs}, M_{UV}^{-21.5}) \propto \int p(EW_{Ly\alpha}^{obs} | EW_{Ly\alpha}^{tran}, x_{HI}, M_{UV}^{-21.5}) p(x_{HI}) p(EW_{Ly\alpha}^{tran} | M_{UV}^{-21.5}) dEW_{Ly\alpha}^{tran}$$

where $p(EW_{Ly\alpha}^{obs} | EW_{Ly\alpha}^{tran}, x_{HI}, M_{UV}^{-21.5})$ is the likelihood of the measured $EW_{Ly\alpha}$ given the neutral fraction, and marginalizing over the values of $EW_{Ly\alpha}^{tran}$. $p(x_{HI})$ is the prior on the global neutral fraction, which we assume to be uniform between $[0,1]$. $p(EW_{Ly\alpha}^{tran} | M_{UV}^{-21.5})$ is the PDF of the transmitted EW computed in the previous section for $M_{UV} = -21.5$. $Ly\alpha$ optical depths vary smoothly with x_{HI} , so we interpolate between our nine simulations to build a function for the $EW_{Ly\alpha}$ distributions dependent on x_{HI} and M_{UV} . We assume that the likelihood of $EW_{Ly\alpha}^{obs}$ is a normal, with known standard deviation that we set equal to the measurement uncertainty provided by Bunker et al. (2023).

We use a Metropolis-Hastings algorithm to sample the posterior, accounting for measurement errors on $EW_{Ly\alpha}$.

3. RESULTS AND DISCUSSION

The main result of our analysis is presented in Figure 3, where we show the x_{HI} posterior in the left panel. Not surprisingly, with only one galaxy, the value of x_{HI} is poorly constrained. However, it is clear that x_{HI} is smaller than 0.88 at 95% confidence level (the 95% credibility region is indicated by the vertical line in Figure 3). In the right panel of Figure 3, we show the constraint on x_{HI} derived from GN-z11 on the reionization history timeline, and compare it with constraints on the neutral fraction from other observations: $Ly\alpha$ EW of galaxies (Mason et al. 2018a, 2019; Hoag et al. 2019); the clustering of $Ly\alpha$ emitter galaxies (Ouchi et al. 2010; Greig et al. 2016); $Ly\alpha$ and $Ly\beta$ dark fraction (McGreer et al. 2015); QSO damping wings (Davies et al. 2018). While the GN-z11 observation does not constrain the absolute value on x_{HI} (one can just as easily say that x_{HI} is > 0.04 with 95%), the fact that the observation is very far back in the expected timeline of reionization offers a lever, allowing one to distinguish between reionization models.

Predicting the redshift evolution of the volume averaged neutral fraction depends on the number of ionizing sources present at each time, their ionizing spectrum, and the ability of ionizing radiation to escape into the IGM. Once these are known, x_{HI} can be computed by solving:

$$\frac{d(1 - x_{HI})}{dt} = \frac{\dot{N}_{ion}}{n_H} - \frac{(1 - x_{HI})}{t_{rec}}, \quad (2)$$

(Madau et al. 1999; Robertson et al. 2013; Ishigaki et al. 2018) where \dot{N}_{ion} is the ionizing photon production rate, n_H is the comoving gas number density, and t_{rec} is the recombination time scale. n_H and t_{rec} are defined as

$$n_H = \frac{X_p \Omega_b \rho_c}{m_H}, \quad (3)$$

$$t_{rec} = [C_{HII} \alpha_B(T) (1 + Y_p/4X_p) n_H (1+z)^3]^{-1}, \quad (4)$$

where X_p , Y_p are the primordial mass fraction of hydrogen and helium, Ω_b is the baryon energy density fraction, ρ_c is the critical density, ($\Omega_b \rho_c = 4.2 \times 10^{-31} [g/cm^3]$), $C_{HII} \equiv \langle n_{HII}^2 \rangle / \langle n_{HII} \rangle^2$ is the clumping factor, and $\alpha_B(T)$ is the case B recombination coefficient. Here we assume $C_{HII} = 3$, and $\alpha_B = 2.6 \times 10^{-13} cm^3 s^{-1}$, for an electron temperature of $10^4 K$. We solve Equation 2 iteratively, assuming the boundary condition that $x_{HI} = 1.0$ at $z = 18$, i.e., we assume that the first sources of ionizing photons appear at this redshift.

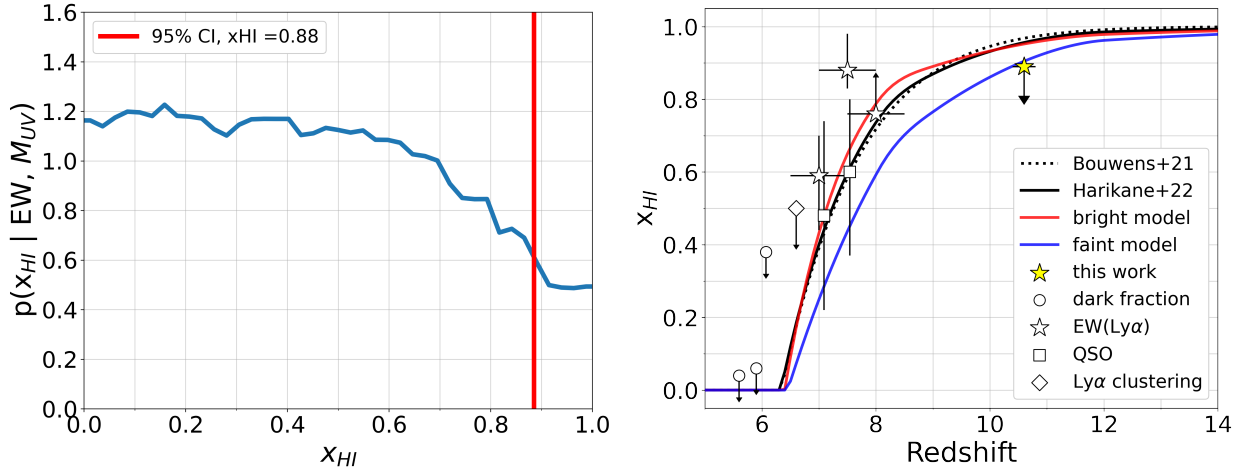


Figure 3. *Left:* the posterior distribution of x_{HI} . *Right:* the reionization history. The dash and solid black lines are constant f_{esc} models with Schechter LF (Bouwens et al. 2021) and double power-law LF (Harikane et al. 2023). The red and blue lines are the models where bright and faint galaxies have higher escape fraction, respectively. The observational constraints are shown in white markers, and the constraint in constraint inferred by GN-z11 is marked as yellow star.

The major uncertainties in the calculation of x_{HI} above are introduced in the ionizing photon production rate, \dot{N}_{ion} , that can be expressed as the product of three components:

$$\dot{N} = f_{\text{esc}} \xi_{\text{ion}} \rho_{\text{UV}}, \quad (5)$$

where f_{esc} is the absolute LyC escape fraction, ξ_{ion} is the ionizing photon production efficiency, and ρ_{UV} is the UV luminosity density, i.e., the integral of the galaxy UV luminosity function (LF).

The UV LF has changed very quickly after JWST observations. Early JWST results indicate that bright galaxies at $z > 8$ are more numerous than previously expected (Finkelstein et al. 2022), and a double power-law LF (as opposed of a classical Schechter LF) was proposed to account for the newly discovered population of bright galaxies (Bouwens et al. 2021; Harikane et al. 2023). Are these new bright sources responsible for the observed neutral fraction at $z = 10.6$? The relative contribution of bright and faint galaxies to the reionization budget is unconstrained. Which objects prevail has an impact on the reionization timeline: reionization starts late but completes rapidly if bright galaxies dominate, (Sharma et al. 2016; Naidu et al. 2020), while it starts early but proceeds slowly if faint galaxies played the major role (Finkelstein et al. 2019).

In what follows we consider four simple reionization history models that include the recent developments in the LF studies and vary the contribution of bright and faint galaxies to the ionizing budget. For all models, we assume $\log(\xi_{\text{ion}}/[\text{Hz erg}^{-1}])=25.7$, characteristic of high-redshift star-forming galaxies (Ning et al. 2023; Tang et al. 2023).

First, we consider the reionization models that assume different luminosity functions at $z > 8$: a Schechter LF (dashed line, Bouwens et al. 2021), and a double power-law LF (solid line; Harikane et al. 2023). At $z \leq 8$, both models are calculated with the Schechter LF in Bouwens et al. (2021). We adopt a constant $f_{\text{esc}}=0.12$ at all redshifts in both models. We find that although there are more UV bright ($M_{\text{UV}} < -22$) galaxies when the double power-law LF is used, the early ($z > 9$) reionization histories are roughly equivalent in the two models. Neither model, however, is able to reionize the universe early enough to account for the x_{HI} upper limit at $z = 10.6$, as in both models x_{HI} reaches 90% only by $z_{90} \approx 9.4$.

Next, we consider the models where bright ($M_{\text{UV}} < -18$) or faint galaxies ($M_{\text{UV}} \geq -18$) dominate the ionizing photon budget. To achieve this goal we vary the escape fraction as a function of both M_{UV} and redshift:

$$f_{\text{esc}} = \begin{cases} 0.08 + 0.022(z - 6) - 0.12(M_{\text{UV}} + 18), & \text{bright} \\ 0.08 + 0.022(z - 6) + 0.02(M_{\text{UV}} + 18), & \text{faint} \end{cases}$$

with flattening at $f_{\text{esc}}=0.5$. We refer to these models as bright and faint models. In both models, we adopt the DP LF from Harikane et al. (2023) at $z > 8$ and the Schechter LF from Bouwens et al. (2021) at $z \leq 8$.

The bright model (red curve in Figure 3) shows a late and rapid reionization similar to the models with constant f_{esc} , despite the fact that the dominant contributors to the ionizing photon budget are different (in the constant f_{esc} models, faint galaxies dominate because of their high space density compared to bright galaxies). In the faint model (blue curve in

Figure 3), the ionizing photon contribution of galaxies with $M_{UV} > -18$ is enhanced with respect to the constant f_{esc} models, causing reionization to start earlier. Specifically, we find that x_{HI} reaches 90% by $z_{90} \approx 10.9$ and progresses more slowly compared to models where brighter galaxies dominate. The faint model is the preferred scenario for the early stage of reionization ($z > 10$) in light of the $x_{\text{HI}} < 0.88$ constraint inferred from GN-z11.

An independent constraint on the reionization history comes from observations of the cosmic microwave background. Recently, *Planck* (Planck-Collaboration et al. 2020) measured the (integrated) optical depth to Thomson scattering to be $\tau = 0.056 \pm 0.007$, ruling out the need of a large contribution from galaxies at $z > 10$, and favoring a fast and late reionization process. The redshift evolution of the free electron fraction, $x_e(z)$, constrained by *Planck*, however, depends on the specific form used to model the reionization history, as τ is only sensitive to the integral of the electron density over time, and not its detailed shape. The FlexKnot model assumed in PlanckCollaboration VI limits the contribution to the optical depth of $z > 15$ galaxies to less than 1%, but leaves space to the possibility that the

universe was not fully neutral at $z = 10.6$, with a free electron fraction of $\approx 8-10\%$, consistent with the upper limit presented here.

4. CONCLUSIONS

At a record distance of $z = 10.6$, GN-z11 is the highest-redshift Ly α -emitting galaxy known, well within the heart of the reionization epoch. We use an inhomogeneous reionization simulation to derive the probability distribution of the transmitted EW $_{\text{Ly}\alpha}$ through the IGM as a function of M_{UV} and the average neutral gas fraction, x_{HI} . We use these distributions to estimate the posterior distribution function on x_{HI} at $z = 10.6$. With data for only one galaxy, we place an upper limit on the global neutral fraction at $z = 10.6$, i.e., $x_{\text{HI}} \lesssim 0.88$ with a probability of 95%. With this constraint we are able to exclude reionization histories dominated by bright galaxies; a scenario wherein faint galaxies have a higher escape fraction of ionizing photons, and so drive reionization, is favored.

Software: *Astropy* (Robitaille et al. 2013), *SciPy* (Oliphant 2007), *NumPy* (van der Walt et al. 2011), and *Matplotlib* (Hunter 2007).

REFERENCES

- Bouwens, R. J., Oesch, P. A., Stefanon, M., et al. 2021, *AJ*, 162, 47, doi: [10.3847/1538-3881/abf83e](https://doi.org/10.3847/1538-3881/abf83e)
- Brinchmann, J. 2022, High-z Galaxies with JWST and Local Analogues – It Is Not Only Star Formation, arXiv. <https://arxiv.org/abs/2208.07467>
- Bruton, S., Scarlata, C., Haardt, F., et al. 2023, arXiv, doi: [10.48550/arXiv.2305.04949](https://doi.org/10.48550/arXiv.2305.04949)
- Bunker, A. J., Saxena, A., Cameron, A. J., et al. 2023, JADES NIRSpec Spectroscopy of GN-z11: Lyman- α Emission and Possible Enhanced Nitrogen Abundance in a $z=10.60$ Luminous Galaxy, arXiv. <https://arxiv.org/abs/2302.07256>
- Cameron, A. J., Saxena, A., Bunker, A. J., et al. 2023, JADES: Probing Interstellar Medium Conditions at $z \sim 5.5-9.5$ with Ultra-Deep JWST/NIRSpec Spectroscopy, arXiv. <https://arxiv.org/abs/2302.04298>
- Choudhury, T. R., Puchwein, E., Haehnelt, M. G., & Bolton, J. S. 2015, *Mon. Not. R. Astron. Soc.*, 452, 261, doi: [10.1093/mnras/stv1250](https://doi.org/10.1093/mnras/stv1250)
- Curtis-Lake, E., Carniani, S., Cameron, A., et al. 2023, Spectroscopic Confirmation of Four Metal-Poor Galaxies at $Z=10.3-13.2$, arXiv. <https://arxiv.org/abs/2212.04568>
- Davies, F. B., Hennawi, J. F., Bañados, E., et al. 2018, *ApJ*, 864, 142, doi: [10.3847/1538-4357/aad6dc](https://doi.org/10.3847/1538-4357/aad6dc)
- De Barros, S., Pentericci, L., Vanzella, E., et al. 2017, *A&A*, 608, A123, doi: [10.1051/0004-6361/201731476](https://doi.org/10.1051/0004-6361/201731476)
- Dijkstra, M. 2014, *Publ. Astron. Soc. Aust.*, 31, e040, doi: [10.1017/pasa.2014.33](https://doi.org/10.1017/pasa.2014.33)
- . 2017, 81
- Fan, X., Strauss, M. A., Becker, R. H., et al. 2006, *AJ*, 132, 117, doi: [10.1086/504836](https://doi.org/10.1086/504836)
- Finkelstein, S. L., D’Aloisio, A., Paardekooper, J.-P., et al. 2019, *ApJ*, 879, 36, doi: [10.3847/1538-4357/ab1ea8](https://doi.org/10.3847/1538-4357/ab1ea8)
- Finkelstein, S. L., Bagley, M. B., Ferguson, H. C., et al. 2022, CEERS Key Paper I: An Early Look into the First 500 Myr of Galaxy Formation with JWST, arXiv. <https://arxiv.org/abs/2211.05792>
- Greig, B., Mesinger, A., & Bañados, E. 2019, *Monthly Notices of the Royal Astronomical Society*, 484, 5094, doi: [10.1093/mnras/stz230](https://doi.org/10.1093/mnras/stz230)
- Greig, B., Mesinger, A., Haiman, Z., & Simcoe, R. A. 2016, *Mon. Not. R. Astron. Soc.*, stw3351, doi: [10.1093/mnras/stw3351](https://doi.org/10.1093/mnras/stw3351)
- Harikane, Y., Ouchi, M., Oguri, M., et al. 2023, *ApJS*, 265, 5, doi: [10.3847/1538-4365/acaaa9](https://doi.org/10.3847/1538-4365/acaaa9)

- Hashimoto, T., Garel, T., Guiderdoni, B., et al. 2017, *A&A*, 608, A10, doi: [10.1051/0004-6361/201731579](https://doi.org/10.1051/0004-6361/201731579)
- Hayes, M. J., & Scarlata, C. 2023, On the Sizes of Ionized Bubbles around the Highest Redshift Galaxies. Spectral Shapes of the Lyman-alpha Emission from Galaxies III, arXiv. <http://ascl.net/arXiv:2303.03160>
- Hoag, A., Bradač, M., Huang, K.-H., et al. 2019, *ApJ*, 878, 12, doi: [10.3847/1538-4357/ab1de7](https://doi.org/10.3847/1538-4357/ab1de7)
- Hu, W., Wang, J., Zheng, Z.-Y., et al. 2019, *ApJ*, 886, 90, doi: [10.3847/1538-4357/ab4cf4](https://doi.org/10.3847/1538-4357/ab4cf4)
- Hunter, J. D. 2007, *Computing in Science & Engineering*, 9, 90, doi: [10.1109/MCSE.2007.55](https://doi.org/10.1109/MCSE.2007.55)
- Ishigaki, M., Kawamata, R., Ouchi, M., et al. 2018, *ApJ*, 854, 73, doi: [10.3847/1538-4357/aaa544](https://doi.org/10.3847/1538-4357/aaa544)
- Jung, I., Finkelstein, S. L., Livermore, R. C., et al. 2018, *ApJ*, 864, 103, doi: [10.3847/1538-4357/aad686](https://doi.org/10.3847/1538-4357/aad686)
- Jung, I., Finkelstein, S. L., Dickinson, M., et al. 2020, *ApJ*, 904, 144, doi: [10.3847/1538-4357/abbd44](https://doi.org/10.3847/1538-4357/abbd44)
- Madau, P., Haardt, F., & Rees, M. J. 1999, *ApJ*, 514, 648, doi: [10.1086/306975](https://doi.org/10.1086/306975)
- Malhotra, S., & Rhoads, J. 2004, *ApJ*, 617, L5, doi: [10.1086/427182](https://doi.org/10.1086/427182)
- . 2006, *ApJ*, 647, L95, doi: [10.1086/506983](https://doi.org/10.1086/506983)
- Mason, C., Trenti, M., & Treu, T. 2015, *ApJ*, 813, 21, doi: [10.1088/0004-637X/813/1/21](https://doi.org/10.1088/0004-637X/813/1/21)
- Mason, C. A., Treu, T., Dijkstra, M., et al. 2018a, *ApJ*, 856, 2, doi: [10.3847/1538-4357/aab0a7](https://doi.org/10.3847/1538-4357/aab0a7)
- Mason, C. A., Treu, T., de Barros, S., et al. 2018b, *ApJ*, 857, L11, doi: [10.3847/2041-8213/aabbab](https://doi.org/10.3847/2041-8213/aabbab)
- Mason, C. A., Fontana, A., Treu, T., et al. 2019, *Monthly Notices of the Royal Astronomical Society*, 485, 3947, doi: [10.1093/mnras/stz632](https://doi.org/10.1093/mnras/stz632)
- McGreer, I., Mesinger, A., & D'Odorico, V. 2015, *Monthly Notices of the Royal Astronomical Society*, 447, 499, doi: [10.1093/mnras/stu2449](https://doi.org/10.1093/mnras/stu2449)
- McGreer, I. D., Mesinger, A., & Fan, X. 2011, *Monthly Notices of the Royal Astronomical Society*, 415, 3237, doi: [10.1111/j.1365-2966.2011.18935.x](https://doi.org/10.1111/j.1365-2966.2011.18935.x)
- Mesinger, A., & Furlanetto, S. 2007, *ApJ*, 669, 663, doi: [10.1086/521806](https://doi.org/10.1086/521806)
- Mesinger, A., Furlanetto, S., & Cen, R. 2011, *Monthly Notices of the Royal Astronomical Society*, 411, 955, doi: [10.1111/j.1365-2966.2010.17731.x](https://doi.org/10.1111/j.1365-2966.2010.17731.x)
- Mesinger, A., Greig, B., & Sobacchi, E. 2016, *Mon. Not. R. Astron. Soc.*, 459, 2342, doi: [10.1093/mnras/stw831](https://doi.org/10.1093/mnras/stw831)
- Morales, A. M., Mason, C. A., Bruton, S., et al. 2021, *ApJ*, 919, 120, doi: [10.3847/1538-4357/ac1104](https://doi.org/10.3847/1538-4357/ac1104)
- Naidu, R. P., Tacchella, S., Mason, C. A., et al. 2020, *ApJ*, 892, 109, doi: [10.3847/1538-4357/ab7cc9](https://doi.org/10.3847/1538-4357/ab7cc9)
- Ning, Y., Cai, Z., Jiang, L., et al. 2023, *The Astrophysical Journal*, 944, L1, doi: [10.3847/2041-8213/acb26b](https://doi.org/10.3847/2041-8213/acb26b)
- Ning, Y., Jiang, L., Zheng, Z.-Y., & Wu, J. 2022, *The Astrophysical Journal*, 926, 230, doi: [10.3847/1538-4357/ac4268](https://doi.org/10.3847/1538-4357/ac4268)
- Oliphant, T. E. 2007, *Computing in Science & Engineering*, 9, 10, doi: [10.1109/MCSE.2007.58](https://doi.org/10.1109/MCSE.2007.58)
- Ono, Y., Ouchi, M., Mobasher, B., et al. 2012, *ApJ*, 744, 83, doi: [10.1088/0004-637X/744/2/83](https://doi.org/10.1088/0004-637X/744/2/83)
- Ouchi, M., Shimasaku, K., Furusawa, H., et al. 2010, *ApJ*, 723, 869, doi: [10.1088/0004-637X/723/1/869](https://doi.org/10.1088/0004-637X/723/1/869)
- Ouchi, M., Harikane, Y., Shibuya, T., et al. 2018, *Publications of the Astronomical Society of Japan*, 70, doi: [10.1093/pasj/psx074](https://doi.org/10.1093/pasj/psx074)
- Pentericci, L., Fontana, A., Vanzella, E., et al. 2011, *ApJ*, 743, 132, doi: [10.1088/0004-637X/743/2/132](https://doi.org/10.1088/0004-637X/743/2/132)
- Planck-Collaboration, Aghanim, N., Akrami, Y., et al. 2020, *A&A*, 641, A6, doi: [10.1051/0004-6361/201833910](https://doi.org/10.1051/0004-6361/201833910)
- Qin, Y., Mesinger, A., Bosman, S. E. I., & Viel, M. 2021, *Monthly Notices of the Royal Astronomical Society*, 506, 2390, doi: [10.1093/mnras/stab1833](https://doi.org/10.1093/mnras/stab1833)
- Rhoads, J. E., & Malhotra, S. 2001, *The Astrophysical Journal*, 563, L5, doi: [10.1086/338477](https://doi.org/10.1086/338477)
- Robertson, B. E., Furlanetto, S. R., Schneider, E., et al. 2013, *ApJ*, 768, 71, doi: [10.1088/0004-637X/768/1/71](https://doi.org/10.1088/0004-637X/768/1/71)
- Robitaille, T. P., Tollerud, E. J., Greenfield, P., et al. 2013, *A&A*, 558, A33, doi: [10.1051/0004-6361/201322068](https://doi.org/10.1051/0004-6361/201322068)
- Schaerer, D., Marques-Chaves, R., Barrufet, L., et al. 2022, *A&A*, 665, L4, doi: [10.1051/0004-6361/202244556](https://doi.org/10.1051/0004-6361/202244556)
- Schroeder, J., Mesinger, A., & Haiman, Z. 2013, *Monthly Notices of the Royal Astronomical Society*, 428, 3058, doi: [10.1093/mnras/sts253](https://doi.org/10.1093/mnras/sts253)
- Sharma, M., Theuns, T., Frenk, C. S., et al. 2016, *Mon. Not. R. Astron. Soc. Lett.*, 458, L94, doi: [10.1093/mnrasl/slw021](https://doi.org/10.1093/mnrasl/slw021)
- Sobacchi, E., & Mesinger, A. 2015, arXiv:1505.02787 [astro-ph]. <https://arxiv.org/abs/1505.02787>
- Stark, D. P., Ellis, R. S., Chiu, K., Ouchi, M., & Bunker, A. 2010, *Monthly Notices of the Royal Astronomical Society*, 408, 1628, doi: [10.1111/j.1365-2966.2010.17227.x](https://doi.org/10.1111/j.1365-2966.2010.17227.x)
- Tang, M., Stark, D. P., Chen, Z., et al. 2023, JWST/NIRSpec Spectroscopy of $z=7-9$ Star Forming Galaxies with CEERS: New Insight into Bright Ly α Emitters in Ionized Bubbles, arXiv. <https://arxiv.org/abs/2301.07072>
- van der Walt, S., Colbert, S. C., & Varoquaux, G. 2011, *Computing in Science & Engineering*, 13, 22, doi: [10.1109/MCSE.2011.37](https://doi.org/10.1109/MCSE.2011.37)

Verhamme, A., Garel, T., Ventou, E., et al. 2018, Monthly Notices of the Royal Astronomical Society: Letters, 478, L60, doi: [10.1093/mnrasl/sly058](https://doi.org/10.1093/mnrasl/sly058)

Whitler, L. R., Mason, C. A., Ren, K., et al. 2020, Monthly Notices of the Royal Astronomical Society, 495, 3602, doi: [10.1093/mnras/staa1178](https://doi.org/10.1093/mnras/staa1178)

Wold, I. G. B., Malhotra, S., Rhoads, J., et al. 2021, arXiv:2105.12191 [astro-ph].
<https://arxiv.org/abs/2105.12191>

Yoshioka, T., Kashikawa, N., Inoue, A. K., et al. 2022, arXiv:2201.07261 [astro-ph].

<https://arxiv.org/abs/2201.07261>